Ultrasensitive Piezoresistive and Piezocapacitive Cellulose-Based Ionic Hydrogels for Wearable Multifunctional Sensing

ACS APPLIED ELECTRONIC MATERIALS

pubs.acs.org/acsaelm Article

Ultrasensitive Piezoresistive and Piezocapacitive Cellulose-Based Ionic Hydrogels for Wearable Multifunctional Sensing

Giorgio Mogli, Annalisa Chiappone, Adriano Sacco, Candido Fabrizio Pirri, and Stefano Stassi*

Cite This: ACS Appl. Electron. Mater. 2023, 5, 205−215 Read Online

ACCESS | Metrics & More | Article Recommendations | Supporting Information

ABSTRACT: Tactile sensors, namely, flexible devices that sense physical stimuli, have received much attention in the last few decades due to their applicability in a wide range of fields like the world of wearables, soft robotics, prosthetics, and e-skin. Nevertheless, achieving a trade-off among stretchability, good sensitivity, easy manufacturability, and multisensing ability is still a challenge. Herein, an extremely flexible strain sensor composed of a cellulose-based hydrogel is presented. A natural biocompatible carboxymethylcellulose (CMC) hydrogel endowed with ionic conductivity by sodium chloride (NaCl) was used as the sensitive part. Both the sensible layer and electrodes were investigated with an innovative approach for wearable sensor applications based on electrochemical impedance spectroscopy to find the best device configuration. The sensor, exploitable both as a piezoresistor and as a piezocapacitor, presents high sensitivity to external stimuli, together with an extreme stretchability of up to 600%, showing the best strain and temperature sensitivity among the ionic conductive hydrogel-based devices presented in the literature. The very high strain sensitivity enables the hydrogel to be implemented in wearable strain sensors to monitor different human motions and physiological signals, representing a valid solution for the realization of transparent, easily manufacturable, and low-environmental-impact devices.

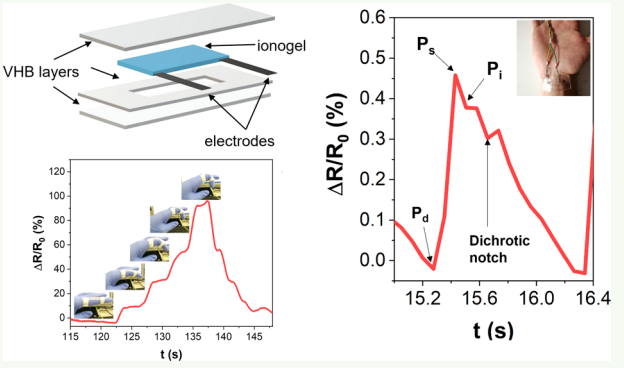

KEYWORDS: *hydrogel, flexible strain sensor, cellulose, piezoresistive, wearable sensor, ionic conductivity*

INTRODUCTION

In recent years, the need to interface the human world with the electronic one has drastically grown. On the one hand, living tissues are characterized by softness, multisensing capacity, self-heal ability, and adaptability. On the other hand, robots and machines are generally stiff and unable to auto-repair. Therefore, devices with intermediate properties are necessary to link the two realms. In this framework, tactile or smart sensors, which are devices able to sense external stimuli, such as deformations, temperature, moisture, and light, could represent an optimal solution. They are designed by mimicking the skin, which is the largest sensor tissue of living beings. The main difference from the traditional sensors is that the smart ones are built exploiting flexible materials in order to be more compliant to the irregular surfaces of soft tissues and robots.[1] This feature makes tactile sensors applicable in a wide range of fields: wearables,[2−4] e-skin,[5−7] prosthetics,[8,9] and soft robotics.[10] As a consequence, the global market of soft tactile sensors has incredibly grown in the last few years.[11] In particular, the reproduction of haptic sensation is a challenge, which still yielded no consolidated results, despite its considerable importance in biomedicine: flexible strain sensors are ideal candidates to overcome this issue.

Hydrogels are intriguing solutions for the production of a sensing-active material since their softness and water-rich environment could overcome the mechanical mismatches between humans and the electronics world.[12] Hydrogels usually possess high transparency and good stretchability without sacrificing conductivity, being water-based materials that can be easily processed. They have been proposed in the form of both electronically and ionically conductive materials for a wide variety of strain sensors.

In electronically conductive hydrogels (ECHs), the current flow is due to mobile electrons. Some polymers, such as polypyrrole, polyaniline (PANI), and poly(3,4-ethylenedioxythiophene):poly(styrene sulfonate), are intrinsically conductive and can be polymerized in situ on a flexible network. Adhikari et al.[13] obtained an interpenetrating PANI-based conductive hydrogel. A swollen poly(vinyl alcohol) (PVA) hydrogel was soaked in an ammonium persulfate (APS)

Received: September 22, 2022
Accepted: December 9, 2022
Published: December 21, 2022

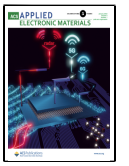

Table 1. Composition of Hydrogels Investigated in This Study (*phr = Per Hundred Resin, Calculated with Respect to the Amount of Polymer)

hydrogel name	NaCl (M)	M-CMC (wt %)	Na-CMC (wt %)	BAPO-OH (phr*)
M-C_2	1	2		2
M-C_3	1	3		2
M-C_4	1	4		2
C_4	1		4	

solution after drying. Then, the gel was submerged in a solution of aniline hydrochloride (AnHCl), and immediately, the polymerization of aniline took place thanks to APS. In this way, PANI was successfully integrated on a flexible substrate, obtaining a gel that could be employed in sensors due to its electrical conductivity. However, the low number of conductive polymers limits their versatility and applicability.[14] In addition, specific synthetic processes are usually required because of their poor solubility, and additional steps need to be carried out to remove cytotoxic unreacted monomers and crosslinkers.[15] Metallic or carbon-based nanomaterials dispersed in polymers networks constitute another solution to endow hydrogels with electronic conductivity. These nanomaterials are usually dispersed in the hydrogel precursor solution and are trapped in the polymeric network after the curing process. Carbon-derived materials, such as carbon nanotubes (CNTs)[4] and graphene oxide (GO),[16] possess outstanding electrical properties and the possibility to be functionalized for promoting adhesion to the polymer. Metal-based nanomaterials are also excellent fillers thanks to their high conductivity. Noble metals are employed in the form of nanoparticles, nanowires, and nanofibers. Chen and co-workers[17] designed an electronically conductive hydrogel by embedding silver-coated copper nanoparticles into gelatin. Therefore, a flexible sensor with excellent mechanical and strain sensitivity properties was manufactured. Although nanomaterial employment improves hydrogel toughness and ensures exceptional conductivity, their homogeneous dispersion is hardly achieved, and the resulting devices are opaque, avoiding visual transmission of information.[18] Moreover, large strains could cause filler dislocation.[14]

Hydrogels can also be doped through ions derived from salts, resulting in ionically conductive hydrogels (ICHs). Ions are dispersed in the precursor solutions, and they can move across the pores of the hydrogel thanks to the water-rich environment. ICH production is usually simpler and cheaper due to the easy availability of doping salts. In addition, despite their lower conductivity compared to ECHs, devices derived from ICHs are usually transparent and their freezing point is lowered thanks to ions, guaranteeing antifreezing property.[19] Therefore, ICHs represent an excellent solution to interface with human skin since they can mimic the flexibility and the ionic conduction typical of living tissues.

Among the different polymers suitable for the production of hydrogels, natural polymers (e.g., cellulose, gelatin, chitosan, alginate, starch, etc.)[20] and their derivatives present several advantages, among which high sustainability, biocompatibility, and biodegradability represent very important features for the development of "green electronic" devices.[21]

Sodium carboxymethylcellulose (Na-CMC) is a common water-soluble cellulose derivate: it is affordable, biocompatible, biodegradable, and FDA-approved. CMC can originate viscous solutions that can also be successfully modified through a methacrylation process, opening the possibility to chemically crosslink the CMC chains thanks to a fast and environmentally friendly photopolymerization reaction.[22] Furthermore, to obtain ionic conductivity, sodium chloride (NaCl) can be employed. Its cheapness, easy availability, and no toxicity make it an ideal candidate for low-environmental-impact ionic conductive systems.

Herein, a sandwich-like tactile sensor composed of a cellulose-based hydrogel encapsulated by a flexible substrate is presented. Neat Na-CMC and chemically crosslinked methacrylated-CMC (M-CMC) were used for the production of hydrogels presenting ionic conductivity thanks to the addition of NaCl to be implemented as a functional material in strain sensors. Electrochemical impedance spectroscopy (EIS) was used for the evaluation of the best electrode material and testing configuration to define the best sensor setup. Finally, the produced sensors were subjected to stretching and bending deformation, showing high sensitivity to external stimuli, if employed both as a piezoresistor and as a piezocapacitor, together with an extreme stretchability of up to 600%. Thanks to the elevated chain mobility of the CMC physical hydrogel, the presented sensors show the best strain and temperature sensitivity with respect to the other ionic conductive hydrogel-based devices presented in the literature. The very high strain sensitivity allows the hydrogel to be implemented into wearable strain sensors to monitor different human motion and physiological signals, representing a valid solution for the realization of transparent, low-cost, eco-friendly, and easily manufacturable devices.

MATERIALS AND METHODS

Materials. Medium-viscosity CMC sodium salt powder and methacrylic anhydride (MW = 154.16) were purchased from Sigma Aldrich (St. Louis, MO). The bismesitoylphosphinic acid (BAPO-OH) photoinitiator[23] was synthesized by Prof. Gruetzmacher's group (ETH Zurich) and kindly provided. Commercial sodium chloride salt was employed as the conductive agent. For the encapsulation of the sensor, VHB 4905 tape (3 M) was used.

Material Preparation and Sensor Fabrication. Methacrylated-CMC (M-CMC) was prepared as described elsewhere.[22] The resulting M-CMC was used for the one-pot preparation of active hydrogels: 1 mol/L NaCl was dissolved in deionized water under magnetic stirring. Then, dried M-CMC was inserted step-by-step under constant magnetic stirring at a temperature of 40 °C until a homogeneous blend was obtained. Concentrations of 2, 3, and 4 wt % M-CMC with respect to DI water were considered. After a gradual cooling to room temperature, the water-soluble photoinitiator (BAPO-OH) was added. The solution was left mixing at room temperature for 5 min and then sonicated (BANDELIN Sonorex Digiplus ultrasonic bath) for 10 min to remove bubbles derived from stirring. In this way, a transparent, homogeneous, and highly viscous solution was obtained. M-CMC hydrogels were formed by exposing the precursor solution to a UV lamp (HAMAMATSU, LC8) for 5 min at 20 mW/cm^2. As a comparison, a gel based on neat Na-CMC was also produced: Na-CMC (4 wt %) was added to the 1 M NaCl solution in DI water and stirred at 40 °C. In this way, cellulose entered the solution and a physical ionogel was achieved without UV light exposure. Lower amounts of Na-CMC were not considered because the final material presented too low viscosity. In addition,

https://doi.org/10.1021/acsaelm.2c01279
ACS Appl. Electron. Mater. 2023, 5, 205−215

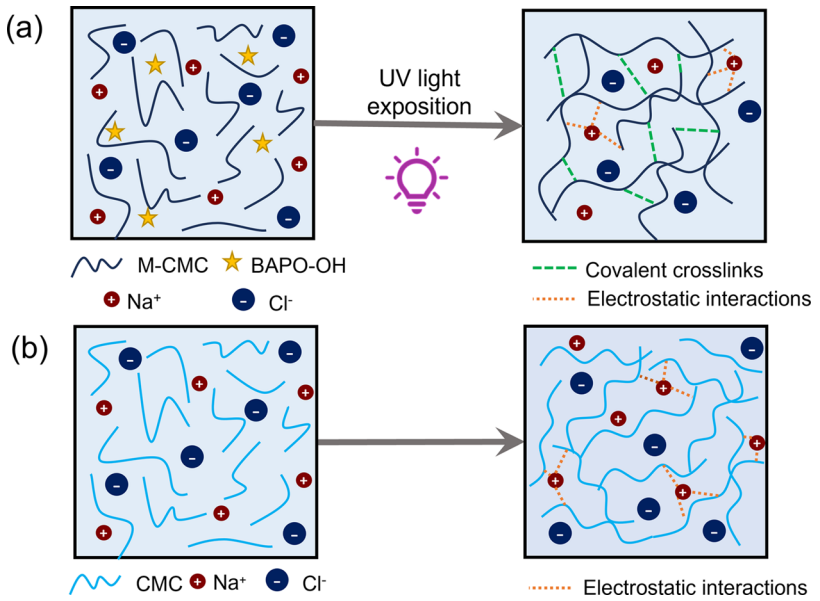

Figure 1. (a) Schematic illustration of M-CMC-based hydrogel production through photopolymerization. (b) Schematic illustration of CMC-based physical hydrogel synthesis.

higher Na-CMC concentrations were avoided due to the difficulty of its solubilization in NaCl 1 M water solution. The prepared samples and their composition are summarized in Table 1.

The tactile sensor was produced by encapsulating the hydrogel with a commercial transparent biadhesive tape (VHB 4905, 3 M) of 0.5 mm thickness. Overlapping three layers of VHB tape, rectangular sensors of 50 × 20 mm^2 area with a sensitive part of 25 × 10 × 0.5 mm^3 were obtained. The hydrogel precursor solution was poured in the cavity obtained by overlapping two layers of a transparent commercial biadhesive tape. A sensitive area of 25 × 10 × 0.5 mm^3 was obtained. Metallic electrodes were inserted in contact with the solution, and the specimen was closed with another sheet of VHB tape after photocuring the precursor solution. Titanium and stainless steel knitted foils as well as stacked sheets of copper-polyimide (PI) and copper-polyimide-copper were investigated as electrode materials. The encapsulation through this transparent tape was required to prevent hydrogel water evaporation, to protect the hydrogel from damage, and to provide a flexible and superstretchable substrate.

Characterization Techniques. Rheological measurements were performed to assess the viscoelastic properties of the materials. Amplitude and sweep tests (frequency ω = 1 Hz) were performed through a rheometer (Physica MCR 302, Anton Paar, Graz, AUT) in the parallel-plate mode varying the amplitude of the strain applied from 0.01 to 1000%.

Electrochemical impedance spectroscopy analyses were performed through a Multi Autolab/M101 (Metrohm) electrochemical working station with the FRA32M module in a two-electrode configuration. A DC voltage of 0.5 V with a superimposed AC voltage of 20 mV was applied, and 10 points for decade were acquired in the frequency range between 0.01 Hz and 100 kHz. Nova software was employed in setting control and data acquisition. The free software EIS spectrum analyzer[24] was used for raw data fitting, using a model composed of a series resistance and two parallels between a resistance and a constant phase element (CPE). The constant phase elements were converted into the corresponding capacitance contributions, as explained in the literature.[25]

The functional analysis of the device was performed by investigating its electrical impedance with an LCR meter (BK precision 894) modeling the device impedance as a parallel between a resistor and a capacitor (R_p and C_p). R_p and C_p were monitored applying a voltage amplitude of 0.5 V and a testing frequency of 1000 Hz. For each point of tensile and temperature tests, static acquisitions of 1 min were made and average values of R_p and C_p were derived. Then, variations of relative resistance and capacitance were computed according to the following formulas

$$\frac{\Delta R}{R_0} = \frac{R - R_0}{R_0} \tag{1}$$

$$\frac{\Delta C}{C_0} = \frac{C - C_0}{C_0} \tag{2}$$

where R and C are the real-time resistance and capacitance and R_0 and C_0 represent the resistance and capacitance when no stimuli are applied, respectively.

Tensile tests were performed in a step-by-step configuration (from 0 to 50% with a 10% step) with a homemade setup, and for each step, electrochemical and electrical measurements were carried out. A tensile machine (Instron) was utilized for dynamic measurements with a speed of 10 mm/min to stretch sensors until their rupture. For cyclic tensile tests, sensors were subjected to 50% strain with a deformation speed of 25 mm/min for 85 subsequent cycles.

For analyzing bending performances, sensors were subjected to different curvature radii (15, 9, 5, 3, and 2.5 cm) thanks to a homemade setup.

Temperature variation sensing tests were carried out inserting hydrogel sensors in an oven (Memmert) and varying the temperature from 25 to 60 °C with a 5 °C step.

Strain sensitivity (S) values in piezoresistive and piezocapacitive modes were computed through the formula

$$S = \frac{\frac{\Delta X}{X_0}(\%)}{\varepsilon(\%)} \tag{3}$$

where X is the electrical parameter considered (resistance or capacitance), X_0 is its value when no strain is applied, and ε is the strain applied to the sample.

Temperature coefficients (TCs) in piezoresistive and piezocapacitive modes were derived from the formula

$$\mathrm{TC} = \frac{\frac{\Delta X}{X_0}(\%)}{\Delta T(^\circ\mathrm{C})} \tag{4}$$

where ΔT is the temperature variation.

https://doi.org/10.1021/acsaelm.2c01279
ACS Appl. Electron. Mater. 2023, 5, 205−215

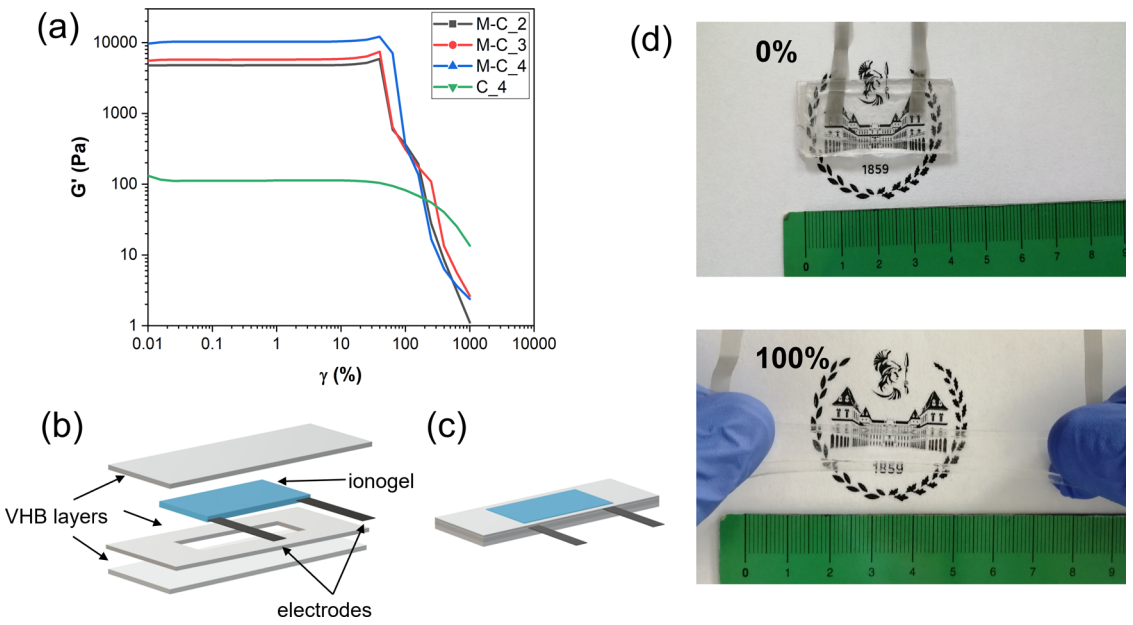

Figure 2. (a) Storage modulus (G') of cellulose-based hydrogels versus shear strain (γ). (b) Exploded view of sensor layers. (c) Model of the assembled sensor. (d) Actual sensor at no applied strain (up) and under 100% of strain (down). The logo of Politecnico di Torino on the back is shown to evidence the transparency of the sensor.

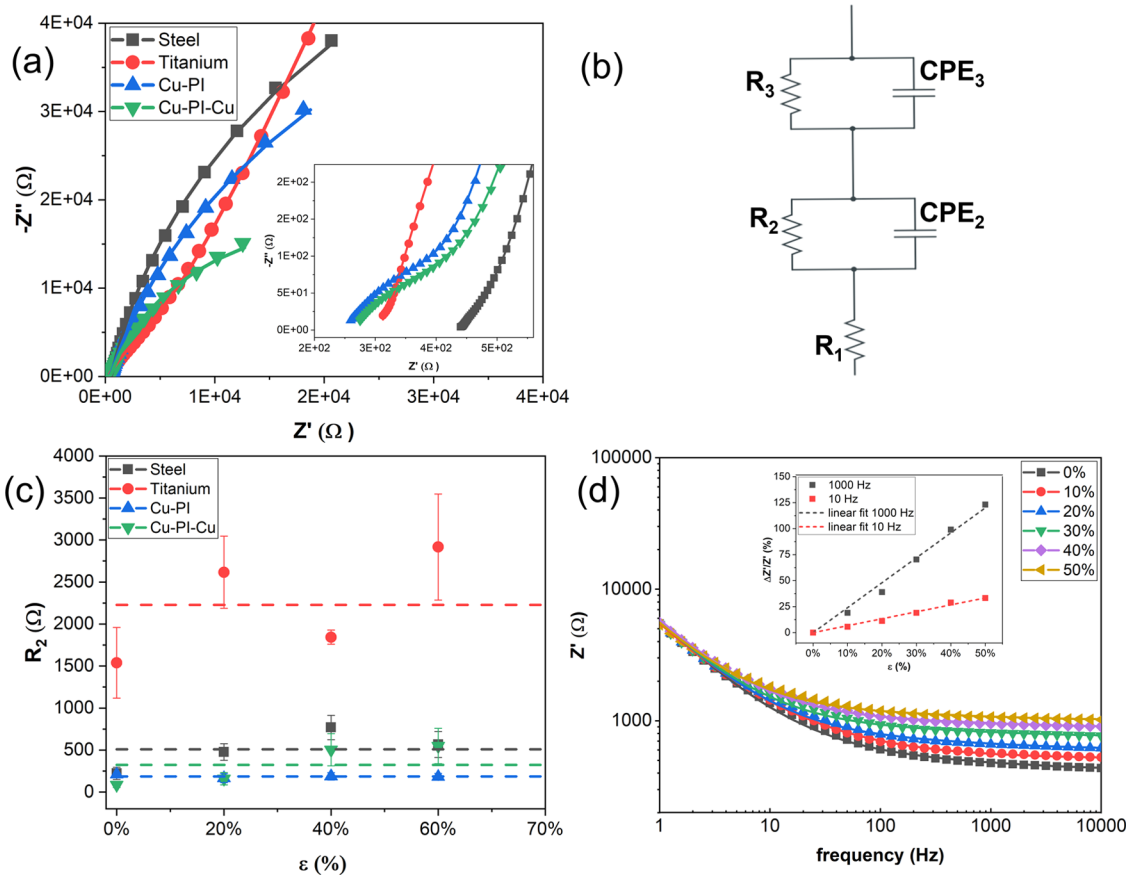

Figure 3. (a) FRA measurements (points) and fitting curves (solid lines) for the four types of electrodes investigated with the sensor made with the M-C_2 hydrogel. In the inset is a zoom over the high-frequency area. (b) Electrical model chosen to fit the data. (c) High-frequency resistance values for sensors with different electrodes subjected to increasing strains. Error bars represent standard deviation regarding a pool of three independent sensors made with the M-C_2 hydrogel. The dashed lines represent the average value of R_2 for electrodes of different electrodes. (d) Real part of impedance variations under an external strain for M-C_2 sensors. The points represent the raw data, and the solid lines represent the fitted data. In the inset are percentage variations of Z' under increasing strain at 10 Hz and 1000 Hz and their linear fitting.

https://doi.org/10.1021/acsaelm.2c01279
ACS Appl. Electron. Mater. 2023, 5, 205−215

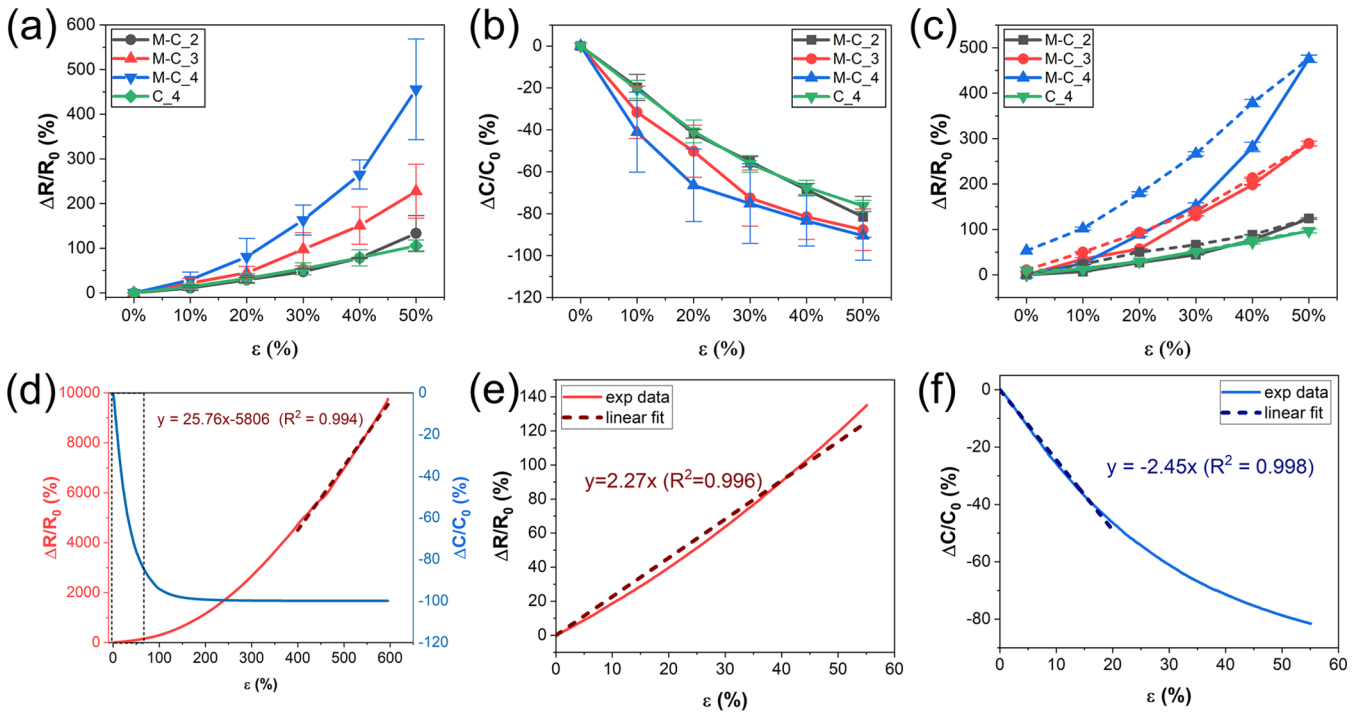

Figure 4. Strain transfer curves of sensors with different hydrogels, tested in (a) the piezoresistive mode and in (b) the piezocapacitive mode. Error bars represent standard deviation regarding a pool of five independent samples. (c) Relative variation of resistance during a cycle of loading (solid line) and unloading (dashed line) for individual samples. (d) Electrical performances of a physical hydrogel-based sensor tested through the tensile machine. Relative variation of resistance and capacitance versus tensile strain. The dashed area is enlarged in the following figures. Zoom-in of the strain range 0−55% of piezoresistive (e) and piezocapacitive (f) transfer curves and their linear fitting.

RESULTS AND DISCUSSION

A one-pot method was exploited to produce the cellulose-based active materials: both Na-CMC and M-CMC were directly solubilized in a 1 M NaCl water solution to obtain the ionically conductive gels (ionogels). Three different concentrations of M-CMC were investigated (see Table 1), and the hydrogels were chemically crosslinked by a fast photopolymerization reaction (Figure 1a). In addition, the behavior of neat Na-CMC was also examined. In this case, the simple presence of electrostatic interactions is expected with the complexation of the Na^+ ions by the COO^- units present on the solubilized CMC chains, leading to the formation of a low-viscosity ionic gel (Figure 1b). Crosslinked hydrogels with various M-CMC concentrations (2, 3, 4%) and the Na-CMC gel were subjected to a rheological amplitude sweep test to gain insights into their mechanical behavior (Figure 2a). The 2 and 3% M-CMC hydrogels show a similar storage modulus and thus comparable stiffness. Instead, the 4% M-CMC ionogel is stiffer than the others due to the higher amount of M-CMC and thus the higher crosslinking density. On the other hand, the 4% Na-CMC hydrogel appears as a viscous colloid solution and, consequently, its storage modulus and stiffness are lower than those of the other samples. Moreover, it is stable in a larger range of deformations since its storage module does not undergo a sharp drop.

Stretchable and transparent strain sensors were assembled using the mentioned hydrogels in a sandwich-like shape in a very easy and quick procedure, as described in the Materials and Methods section (Figure 2b−d).

The electrical behavior of these sensors was then analyzed through EIS.[26] The goal of this analysis was to select the best conductive material to be used as the electrode and the frequency of the electrical stimulus to study our sensors. Typical impedance spectra of the sensors with different electrodes without applied strains are reported in Figure 3a, in which the experimental data are superimposed with fitted data from the theoretical model displayed in Figure 3b. This equivalent circuit worked well for all types of electrodes since fitting curves match well at both high and low frequencies, as shown in the Nyquist plot. The values of the different electrical parameters were extracted from the model. After the conversion of the CPE in the corresponding capacitance contributions (C_2 and C_3), electrical parameter analysis under different external strains enabled the choice of the electrode material, which ensured the highest sensitivity to external strain. The series resistance (R_1) represents the resistance of the contacts and the electrolyte and tends to increase with the applied strain for all kinds of sensors. In fact, under stretching, the ions traverse a longer path because the distance between electrodes increases. The parallel constituted by R_3 and C_3 constitutes the charge diffusion contribution, which has an important role at low frequencies. Instead, the parallel R_2−C_2, which predominates at high frequencies, represents the electrode−electrolyte interface. After this initial analysis, devices with copper-based electrodes (Cu-PI and Cu-PI-Cu) were discarded due to a trace of corrosion at the interface between copper and the hydrogel, thus leading to the consequent instability of the electrical properties. Corrosion of the electrodes was ascribed to the high water content of hydrogels. Finally, since the contribution by the electrode mainly concerns the parallel at higher electrical frequencies (R_2, C_2), stainless steel was selected as a conductive material because it shows an average lower electrical resistance (R_2)

https://doi.org/10.1021/acsaelm.2c01279
ACS Appl. Electron. Mater. 2023, 5, 205−215

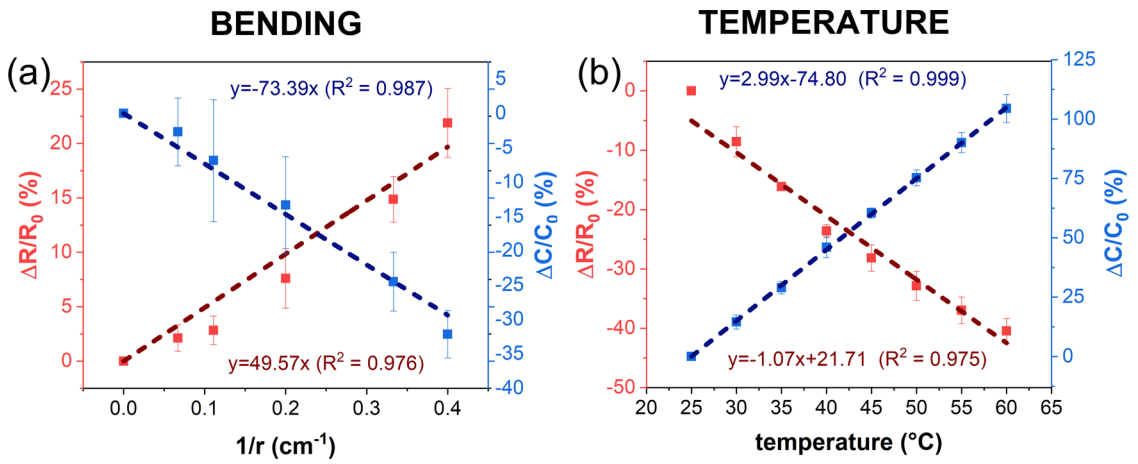

Figure 5. (a) Bending and (b) temperature transfer curves of sensors with the physical hydrogel in piezoresistive (red line) and piezocapacitive (blue line) modes. Error bars represent standard deviation regarding a pool of three independent samples.

with respect to titanium, under all of the investigated strains (Figure 3c).

The EIS technique was then used on the sensors based on different hydrogels and prepared with steel electrodes to find out the best electrical frequency for testing these devices. Each sample was tested at rest and subjected to 10, 20, 30, 40, and 50% of tensile strains. From the analyses of the impedance real part versus frequency, it appears that choosing high frequencies for the electrical testing signal is preferable because the difference between the curve at rest and the curves under different strains is greater than at lower frequencies, as shown for the M-C_2 sensor in Figure 3d. A similar behavior is exhibited by all of the samples, as shown in Figure S1 in the Supporting Information. Therefore, the following analysis on the hydrogel sensors was conducted employing a testing electrical signal with a frequency of 1 kHz.

After assessing the best electrode material and testing frequency, the tensile strain sensitivity of devices with different hydrogel compositions was statically tested in the range from 0 to 50% with a step of 10%. The relative variations of electrical parameters, parallel resistance, and parallel capacitance (R_p and C_p) with respect to their values at the unstrained condition (R_{p0} and C_{p0}) were plotted versus the applied strain (Figure 4a,b). In general, the electrical resistance increases as the strain rises because the distance between the electrodes increases and the polymeric network shrinks, hindering the ions' movement. On the other hand, when a tensile strain is applied, the parallel capacitance decreases due to the increase of the dielectric layer thickness, namely, the distance between electrodes.

The developed sensors demonstrated high sensitivity both as piezoresistors and as piezocapacitors, with both electrical parameters (R and C) being strongly influenced by the applied strain and deformation, making the devices extremely versatile for different final applications. In particular, electrical resistance shows the highest sensitivity to external strain. Furthermore, device sensitivity is strongly dependent on the M-CMC concentration: the higher the M-CMC concentration, the larger the variation of both the electrical parameters in response to applied strains (Figure 4a,b). Moreover, the devices produced with the chemically crosslinked hydrogels show a higher sensitivity with respect to the Na-CMC hydrogel (C_4), which, despite the polymer concentration of 4 wt %, presents a behavior similar to the crosslinked hydrogel with a lower concentration (M-C_2). Nevertheless, the C_4 sample showed clear advantages in terms of reproducibility and measurement repeatability. In Figure 4c, it is clear that in C_4 samples, loading and unloading stretching curves are more similar than those of the other sensors for each strain step and a residual relative resistance variation of about 8% is achieved at no strain applied. In fact, chemically crosslinked gels present at the same time higher stiffness but also brittleness, and this can easily lead the gel to irreversible rupture upon a certain strain, affecting the reproducibility of samples with the same hydrogel. The variability of devices with chemically crosslinked hydrogels is greater, as shown by the higher error bars in Figure 4a,b. Hence, during tensile deformations, rupture processes generate regions in the hydrogel with no electrical conductivity. The combination of the hydrogel deformations and crack formation results in greater variations of electrical resistance and capacitance, as previously seen and reported in similar hydrogel-based strain sensors.[27] On the counterpart, since these nonconductive regions increase the variability in the sensor response, error bars are broader. After a deformation cycle, all of the sensors with M-CMC hydrogels were visually damaged, with clear fractures perpendicular to the strain direction (Figure S3). This effect was observed on the electrical response of the sensors by first increasing the strains and then gradually diminishing the deformations, following the same steps as in the ascent part (Figure 4c). It is evident that devices with 3 and 4% M-CMC did not hold reversible properties after the deformations. This is caused by the phenomenon described earlier. Instead, the relative variation of resistance of the Na-CMC hydrogel recovers almost perfectly since the polymeric network is more flexible and composed of easily restorable electrostatic interactions. Hence, the implementation of hydrogels that are not chemically crosslinked is preferable in the production of sensors with stable electrical properties despite their sensitivity to external strains being lower. For this reason, further measurements of the presented work were conducted on a device composed of the Na-CMC hydrogel. The strain sensitivity of the selected sensor was also explored on the complete sustainable deformation range, applying a dynamic tensile strain through a mechanical testing machine while extracting the electrical parameter variation. Both piezoresistive and piezocapacitive transfer curves were obtained (Figure 4d). This sensor holds an outstanding stretchability, and it can be deformed until six times its initial length without rupture

https://doi.org/10.1021/acsaelm.2c01279
ACS Appl. Electron. Mater. 2023, 5, 205−215

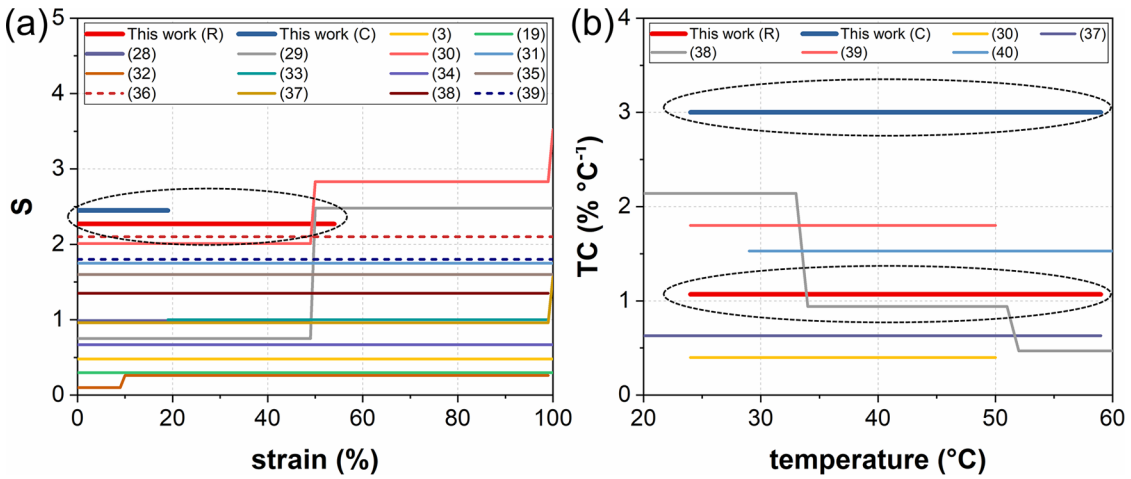

Figure 6. (a) Comparison of strain sensitivity among the sensors of this work (highlighted by the dashed ellipse), in both piezoresistive and piezocapacitive modes, and ionically conductive sensors in the literature reported in Table S1.[3,19,28−39] For devices with no constant sensitivity, their maximum sensitivity is presented through dashed lines. (b) Comparison of temperature sensitivity (temperature coefficient, TC) among the sensors in this work (highlighted by the dashed ellipsis), in both piezoresistive and piezocapacitive modes, and ionically conductive sensors in the literature reported in Table S1.[30,37−40]

(Figure S2). In this wide range of strains, it also shows electrical responsiveness. In the standard strain range involved in human motion (0−55% of strain),[28] it has a quasi-linear transfer curve with a strain sensitivity of 2.27 considering the piezoresistive mode (Figure 4e). On the other hand, the capacitance transfer curve could be approximated by a linear fitting only in the range between 0 and 20% deformation, with a sensitivity of about 2.45. However, the linear model does not work well in a wider range of deformations, as shown in Figure 4f. For higher strains, resistance variations could be approximated by a straight line from 400% strain to 600% strain. In this case, strain sensitivity is much higher than for lower strains, reaching an excellent value of 25.76. Instead, capacitance does not vary anymore for a high deformation range (over 100%), showing that the sensor is unresponsive to elevated deformation in the piezocapacitive mode (Figure 4d). Therefore, the piezoresistive mode is preferable to sense axial strain stimuli because of the higher sensitivity and wider working range. The piezoresistive response was also studied under cyclic deformations. The C_4 sensor showed good repeatability over 80 successive cycles at 50% strain (Figure S4). Despite the presence of a mild drift, attributable to the viscoelastic properties of the VHB tape used for encapsulation, the electrical signal maintains a repeatable amplitude among the cycles (enlargement in Figure S4). Therefore, response stability and durability, key features in wearable applications, are achieved.

Similarly, sensor response to bending deformations was also tested. A homemade bending setup (Figure S5) was employed to deform devices with decreasing curvature radii (15, 9, 5, 3, and 2.5 cm). The relative variations of electrical parameters (R_p and C_p) with respect to their values in the undeformed state (R_{p0} and C_{p0}) were plotted versus the reciprocal of the curvature radii (Figure 5a). Both resistance and capacitance show a quasi-linear behavior. The resistance increases and the capacitance decreases as the bending becomes greater, a behavior similar to the one found with stretching stimuli. Indeed, bending movement is a combination of tensile deformation, on one sample side, and compressive deformation, on the other side; thus, from the experimental data, it is seen that in these sensors the tensile deformation is dominant during the bending process. Comparing the piezoresistive and piezocapacitive transduction methods for sensors made with the Na-CMC hydrogel, there are no consistent differences between them in this range of curvature radii, although capacitance variations are slightly higher in absolute value (Figure 5a). Therefore, either could be exploited as transduction mechanisms.

Furthermore, the dependency of sensor properties on the temperature was evaluated in the RT (25 °C) to 60 °C range. The electrical resistance exhibits a negative quasi-linear relationship with respect to temperature rise (Figure 5b). In fact, when the temperature increases, the mobility of the ions becomes higher, and thus, ionic conductivity is boosted. Simultaneously, the VHB encapsulation dilates, causing changes in device geometry. These combined effects result in an electrical resistance decrease with a sensitivity of about −1% $°C^{-1}$. On the other hand, capacitance shows a positive linear temperature dependency with an increase of temperature due to both geometric effect and electrolyte property variations. In this case, sensitivity measures about 3% $°C^{-1}$, which is higher than the resistance thermal sensitivity. Therefore, the capacitive transduction method is preferable for temperature measurements owing to its excellent linearity and superior sensitivity.

This analysis suggests that the C_4 hydrogel-based device presented in this work could also be employed in temperature sensing. However, since both deformation and thermal stimuli affect the electrical parameters of the sensors, the measurements of strain and temperature at the same time are complex and the two contributions have to be separated. Analytical techniques involving the use of dummy sensors, mounted in regions insensitive to external stimuli, have been widely employed in different sensor applications and could represent a way to implement this device for the simultaneous detection of both temperature and deformation.

To compare the electrical performances of the Na-CMC hydrogel-based sensor, an analysis of the recent ionic conductive hydrogel-based devices presented in the literature has been conducted. In particular, the analysis was focused on

https://doi.org/10.1021/acsaelm.2c01279
ACS Appl. Electron. Mater. 2023, 5, 205−215

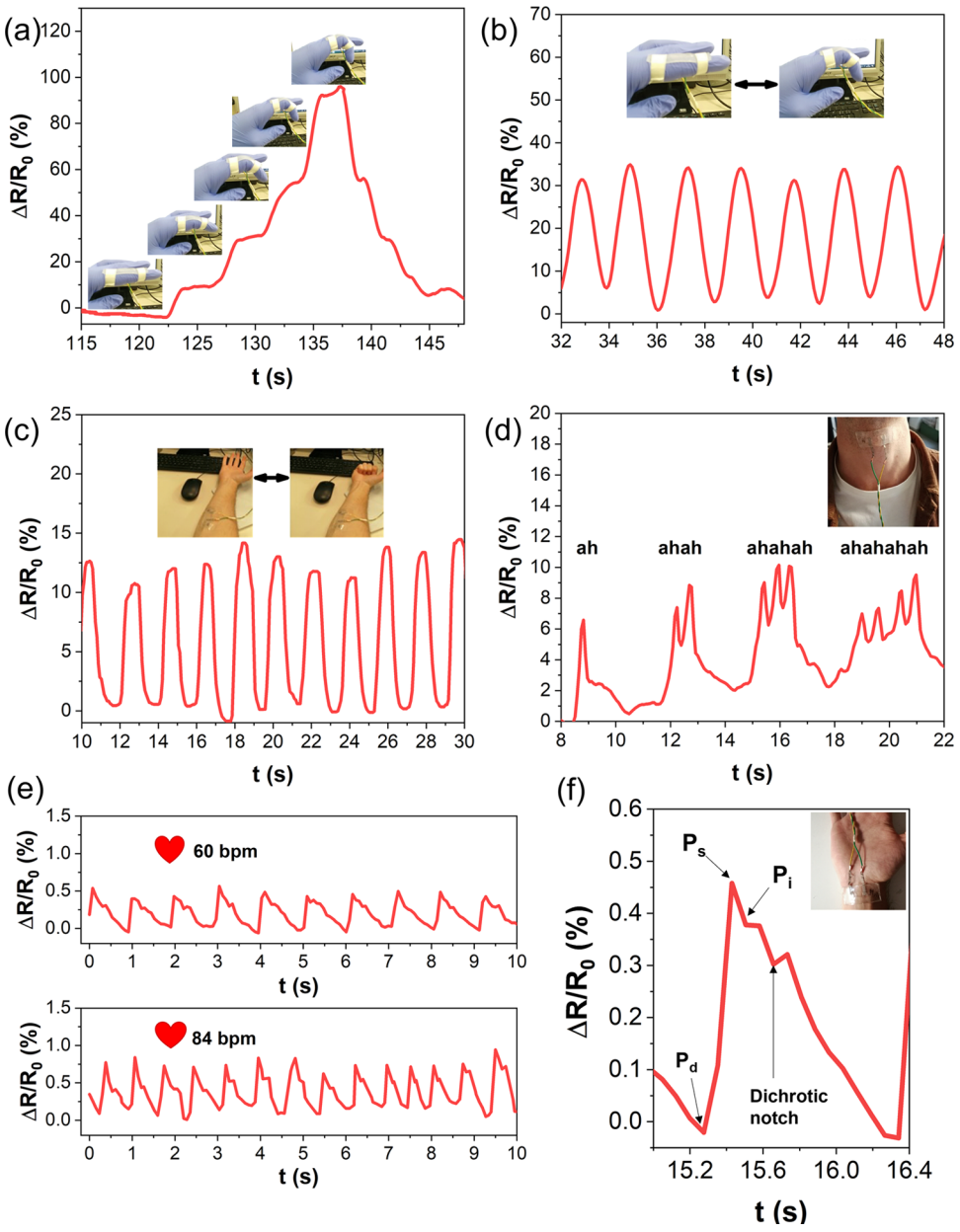

Figure 7. Main biosignals sensed by the M-CMC physical hydrogel-based sensor. (a) Relative resistance variations under different finger bending angles, (b) different bending cycles of the forefinger. (c) Detection of fingers muscular flexors activity during hand closing. (d) Monitoring of vocal cord vibrations when "ah", "ahah", "ahahah", and "ahahahah" are pronounced. (e) Pulse rate at rest (top) and after physical activity (down). (f) Single pulse magnification with the main waveform features (P_d = diastolic pressure, P_s = systolic pressure, P_i = inflection point) as mentioned in the literature.[42]

the electrical resistance and capacitance variations under tensile deformation and at different temperatures (Table S1) where the cellulose hydrogel-based sensor presented in this work shows the best performances. It is worth noting that the piezoresistive device introduced here shows one of the highest strain sensitivity values (Figure 6a) in the strain range involved in human motion (0−55%). The performances of this sensor are reached only by gelatin-based[29] and chitosan-based[30] organohydrogel devices, but in a range above 50%. However, for very high strains (over 400%), this sensor owns superior strain sensitivity (S = 25.76). Regarding the temperature-sensing ability of the capacitive signal, the device shows the highest sensitivity in the range between 25 °C and 60 °C among the sensors presented in the literature (Figure 6b).

These outstanding performances show that CMC-based devices can be successfully employed in the biomedical field as biometric sensors for both deformation and temperature variation sensing. As a demonstration, Na-CMC hydrogel-based sensors were applied in some examples of biomonitoring, exploiting the piezoresistive transduction mode to convert the mechanical deformations into electrical signals. First, detection of human joint motion was investigated by attaching the sensor to the forefinger and bending it. The finger was then bent step by step at different angles (insets in Figure 7a). Consequently, the resistance gradually increased, and when the finger was held at a certain angle, it remained stable (Figure 7a). Moreover, subsequent bending cycles were performed, and the sensor showed an optimal repeatability compatible

https://doi.org/10.1021/acsaelm.2c01279
ACS Appl. Electron. Mater. 2023, 5, 205−215

with the ability of the user to exactly repeat the same movement (Figure 7b). Since the finger movement could be detected, the sensor can certainly be applied for sensing motion of other joints, such as the elbow or the knee. Additionally, the sensor was applied on the muscular flexors of the fingers, located in the forearm, and the hand was repeatedly opened and closed (insets of Figure 7c). The resistance pattern shown in Figure 7c demonstrates that the device can sense deformations caused by muscle contraction. Even in this case, good repeatability of the resistance signal was achieved. In addition, when the sensor was stuck on the throat of a patient (inset of Figure 7d), it could even measure the vibration of vocal cords while speaking. In Figure 7d, laughers of different durations are recognized; whenever "ah" is pronounced, a peak in the resistance signal is recorded. These findings suggest that this tactile sensor could be employed in real-time speech detection instead of microphones, which are unreliable in overcrowded environments.[41]

The sensor was also attached on the wrist of an adult male for sensing the peripheral pulse wave to prove its potential applicability in real-time health monitoring. A first acquisition was done with the patient at rest (Figure 7e up). Then, another trial was performed after mild physical activity (Figure 7e down). The sensor was kept attached in the same position. Comparing the signal before and after the exercise, the heartbeat rate was extracted, increasing from 60 to 84 beats per minute. Moreover, it is possible to find similarities with the classic pulse wave shape in the radial artery, as shown in Figure 7f (right). Typical peaks and valleys are distinguishable. Therefore, it is possible to apply this sensor as a noninvasive method to continuously monitor the pulse rate and to extract from the pulse waves several cardiovascular parameters, helpful in disease diagnosis and prognostic.[11]

All of these results prove the possible application of physical CMC hydrogel-based sensors in various biomedical fields, like continuous health monitoring, detection of muscular activities, and joint motions. The devices show good versatility, being able to perceive both large and subtle deformations.

CONCLUSIONS

In summary, here, a flexible, transparent, cheap, and ultra-stretchable tactile sensor based on a green hydrogel is investigated. A facile one-pot method is used to prepare the ionically conductive CMC hydrogel, in which physical interactions between chains are achieved through sodium chloride salt dispersed in the precursor solution, also providing the ionic conductivity. The sensitive CMC hydrogel-based part was enclosed between shells of a viscoelastic commercial tape in a sandwich-like configuration. Two metallic electrodes were placed in contact with the hydrogel to provide the electrical connection with the external environment. Application of EIS allowed the choice of the electrode material and the sensor's testing frequency, which ensured the best sensitivity to external deformations. In this way, we developed an easy-to-manufacture flexible sensor endowed with transparency, superstretchability (up to 600%), reproducibility, and good sensitivity to external strain (resistive strain gauge of 2.27 in the range between 0 and 100% strains) and to temperature variations (capacitive temperature coefficient of 3% $°C^{-1}$ between 25 and 60 °C). In addition, this sensor could be interestingly applied in both piezoresistive and piezocapacitive modes due to the good performances of the two transduction methods. The demonstration of the CMC hydrogel-based sensor's monitoring abilities for different biosignals, among which joint motion, heart rate, vocal cord vibrations, and surface muscle contraction, could pave the way to its further application in wearables, soft robotics, and prosthetics.

ASSOCIATED CONTENT

Supporting Information

The Supporting Information is available free of charge at https://pubs.acs.org/doi/10.1021/acsaelm.2c01279.

Graph of the real part of impedance variations under external strain for all of the sensors; stress−strain curve of the C_4 sensor and resistance variation of the C_4 sensor under cyclic deformation; images of sensors after a tensile stress cycle and of the bending test setup; and table with all of the details of literature articles cited in Figure 6 of the manuscript (PDF)

AUTHOR INFORMATION

Corresponding Author

Stefano Stassi − *Department of Applied Science and Technology, Politecnico di Torino, 10129 Turin, Italy;* orcid.org/0000-0002-1134-7224; Phone: +39 011 0907394; Email: stefano.stassi@polito.it

Authors

Giorgio Mogli − *Department of Applied Science and Technology, Politecnico di Torino, 10129 Turin, Italy*

Annalisa Chiappone − *Department of Chemical and Geological Sciences (DSCG), University of Cagliari, 09042 Monserrato, Italy;* orcid.org/0000-0003-4651-1140

Adriano Sacco − *Center for Sustainable Future Technologies @Polito, Istituto Italiano di Tecnologia, 10144 Turin, Italy;* orcid.org/0000-0002-9229-2113

Candido Fabrizio Pirri − *Department of Applied Science and Technology, Politecnico di Torino, 10129 Turin, Italy; Center for Sustainable Future Technologies @Polito, Istituto Italiano di Tecnologia, 10144 Turin, Italy*

Complete contact information is available at: https://pubs.acs.org/10.1021/acsaelm.2c01279

Notes

The authors declare no competing financial interest.

ACKNOWLEDGMENTS

This research was partly supported by the Ministero dell'Istruzione, dell'Università e della Ricerca (MIUR), through PRIN2017 - Prot.20172TZHYX grant.

REFERENCES

(1) Stassi, S.; Cauda, V.; Canavese, G.; Pirri, C. F. Flexible Tactile Sensing Based on Piezoresistive Composites: A Review. *Sensors* **2014**, *14*, 5296−5332.

(2) Huang, F.; Wei, W.; Fan, Q.; Li, L.; Zhao, M.; Zhou, Z. Super-Stretchable and Adhesive Cellulose Nanofiber-Reinforced Conductive Nanocomposite Hydrogel for Wearable Motion-Monitoring Sensor. *J. Colloid Interface Sci.* **2022**, *615*, 215−226.

(3) Liu, Y. J.; Cao, W. T.; Ma, M. G.; Wan, P. Ultrasensitive Wearable Soft Strain Sensors of Conductive, Self-Healing, and Elastic Hydrogels with Synergistic "Soft and Hard" Hybrid Networks. *ACS Appl. Mater. Interfaces* **2017**, *9*, 25559−25570.

(4) Xia, S.; Song, S.; Jia, F.; Gao, G. A Flexible, Adhesive and Self-Healable Hydrogel-Based Wearable Strain Sensor for Human Motion

and Physiological Signal Monitoring. *J. Mater. Chem. B* **2019**, *7*, 4638−4648.
(5) Shao, C.; Wang, M.; Meng, L.; Chang, H.; Wang, B.; Xu, F.; Yang, J.; Wan, P. Mussel-Inspired Cellulose Nanocomposite Tough Hydrogels with Synergistic Self-Healing, Adhesive, and Strain-Sensitive Properties. *Chem. Mater.* **2018**, *30*, 3110−3121.
(6) Lei, Z.; Wang, Q.; Sun, S.; Zhu, W.; Wu, P. A Bioinspired Mineral Hydrogel as a Self-Healable, Mechanically Adaptable Ionic Skin for Highly Sensitive Pressure Sensing. *Adv. Mater.* **2017**, *29*, No. 1700321.
(7) Sun, J. Y.; Keplinger, C.; Whitesides, G. M.; Suo, Z. Ionic Skin. *Adv. Mater.* **2014**, *26*, 7608−7614.
(8) Kim, J.; Lee, M.; Shim, H. J.; Ghaffari, R.; Cho, H. R.; Son, D.; Jung, Y. H.; Soh, M.; Choi, C.; Jung, S.; Chu, K.; Jeon, D.; Lee, S. T.; Kim, J. H.; Choi, S. H.; Hyeon, T.; Kim, D. H. Stretchable Silicon Nanoribbon Electronics for Skin Prosthesis. *Nat. Commun.* **2014**, *5*, No. 5747.
(9) Abd, M. A.; Paul, R.; Aravelli, A.; Bai, O.; Lagos, L.; Lin, M.; Engeberg, E. D. Hierarchical Tactile Sensation Integration from Prosthetic Fingertips Enables Multi-Texture Surface Recognition†. *Sensors* **2021**, *21*, No. 4324.
(10) Pang, Y.; Xu, X.; Chen, S.; Fang, Y.; Shi, X.; Deng, Y.; Wang, Z. L.; Cao, C. Skin-Inspired Textile-Based Tactile Sensors Enable Multifunctional Sensing of Wearables and Soft Robots. *Nano Energy* **2022**, *96*, No. 107137.
(11) Kumar, V. S.; Krishnamoorthi, C. Development of Electrical Transduction Based Wearable Tactile Sensors for Human Vital Signs Monitor: Fundamentals, Methodologies and Applications. *Sens. Actuators, A* **2021**, *321*, No. 112582.
(12) Yuk, H.; Lu, B.; Zhao, X. Hydrogel Bioelectronics. *Chem. Soc. Rev.* **2019**, *48*, 1642−1667.
(13) Adhikari, S.; Banerji, P. Polyaniline Composite by in Situ Polymerization on a Swollen PVA Gel. *Synth. Met.* **2009**, *159*, 2519−2524.
(14) Tang, L.; Wu, S.; Qu, J.; Gong, L.; Tang, J. A Review of Conductive Hydrogel Used in Flexible Strain Sensor. *Materials* **2020**, *13*, No. 3947.
(15) Xu, J.; Tsai, Y. L.; Hsu, S. H. Design Strategies of Conductive Hydrogel for Biomedical Applications. *Molecules* **2020**, *25*, No. 5296.
(16) Jing, X.; Mi, H. Y.; Peng, X. F.; Turng, L. S. Biocompatible, Self-Healing, Highly Stretchable Polyacrylic Acid/Reduced Graphene Oxide Nanocomposite Hydrogel Sensors via Mussel-Inspired Chemistry. *Carbon* **2018**, *136*, 63−72.
(17) Chen, K.; Hu, Y.; Liu, M.; Wang, F.; Liu, P.; Yu, Y.; Feng, Q.; Xiao, X. Highly Stretchable, Tough, and Conductive Ag@Cu Nanocomposite Hydrogels for Flexible Wearable Sensors and Bionic Electronic Skins. *Macromol. Mater. Eng.* **2021**, *306*, No. 2100341.
(18) Han, L.; Yan, L.; Wang, M.; Wang, K.; Fang, L.; Zhou, J.; Fang, J.; Ren, F.; Lu, X. Transparent, Adhesive, and Conductive Hydrogel for Soft Bioelectronics Based on Light-Transmitting Polydopamine-Doped Polypyrrole Nanofibrils. *Chem. Mater.* **2018**, *30*, 5561−5572.
(19) Tong, R.; Chen, G.; Pan, D.; Tian, J.; Qi, H.; Li, R.; Lu, F.; He, M. Ultrastretchable and Antifreezing Double-Cross-Linked Cellulose Ionic Hydrogels with High Strain Sensitivity under a Broad Range of Temperature. *ACS Sustainable Chem. Eng.* **2019**, *7*, 14256−14265.
(20) Gyles, D. A.; Castro, L. D.; Silva, J. O. C.; Ribeiro-Costa, R. M. A Review of the Designs and Prominent Biomedical Advances of Natural and Synthetic Hydrogel Formulations. *Eur. Polym. J.* **2017**, *88*, 373−392.
(21) Li, W.; Liu, Q.; Zhang, Y.; Li, C.; He, Z.; Choy, W. C. H.; Low, P. J.; Sonar, P.; Kyaw, A. K. K. Biodegradable Materials and Green Processing for Green Electronics. *Adv. Mater.* **2020**, *32*, No. 2001591.
(22) Melilli, G.; Carmagnola, I.; Tonda-Turo, C.; Pirri, F.; Ciardelli, G.; Sangermano, M.; Hakkarainen, M.; Chiappone, A. DLP 3D Printing Meets Lignocellulosic Biopolymers: Carboxymethyl Cellulose Inks for 3D Biocompatible Hydrogels. *Polymers* **2020**, *12*, No. 1655.
(23) Beil, A.; Müller, G.; Käser, D.; Hattendorf, B.; Li, Z.; Krumeich, F.; Rosenthal, A.; Rana, V. K.; Schönberg, H.; Benkő, Z.; Grützmacher, H. Bismesitoylphosphinic Acid (BAPO-OH): A Ligand for Copper Complexes and Four-Electron Photoreductant for the Preparation of Copper Nanomaterials. *Angew. Chem., Int. Ed.* **2018**, *57*, 7697−7702.
(24) Bondarenko, A. S.; Ragoisha, G. A.EIS spectrum analyser. http://www.abc.chemistry.bsu.by/vi/analyser/.
(25) Sacco, A. Electrochemical Impedance Spectroscopy: Fundamentals and Application in Dye-Sensitized Solar Cells. *Renewable Sustainable Energy Rev.* **2017**, *79*, 814−829.
(26) Stassi, S.; Sacco, A.; Canavese, G. Impedance Spectroscopy Analysis of the Tunnelling Conduction Mechanism in Piezoresistive Composites. *J. Phys. D: Appl. Phys.* **2014**, *47*, No. 345306.
(27) Huang, J.; Peng, S.; Gu, J.; Chen, G.; Gao, J.; Zhang, J.; Hou, L.; Yang, X.; Jiang, X.; Guan, L. Self-Powered Integrated System of a Strain Sensor and Flexible All-Solid-State Supercapacitor by Using a High Performance Ionic Organohydrogel. *Mater. Horiz.* **2020**, *7*, 2085−2096.
(28) Zeng, S.; Zhang, J.; Zu, G.; Huang, J. Transparent, Flexible, and Multifunctional Starch-Based Double-Network Hydrogels as High-Performance Wearable Electronics. *Carbohydr. Polym.* **2021**, *267*, No. 118198.
(29) Wu, M.; Wang, X.; Xia, Y.; Zhu, Y.; Zhu, S.; Jia, C.; Guo, W.; Li, Q.; Yan, Z. Stretchable Freezing-Tolerant Triboelectric Nanogenerator and Strain Sensor Based on Transparent, Long-Term Stable, and Highly Conductive Gelatin-Based Organohydrogel. *Nano Energy* **2022**, *95*, No. 106967.
(30) Gao, Y.; Jia, F.; Gao, G. Ultra-Thin, Transparent, Anti-Freezing Organohydrogel Film Responded to a Wide Range of Humidity and Temperature. *Chem. Eng. J.* **2022**, *430*, No. 132919.
(31) Hussain, I.; Ma, X.; Luo, Y.; Luo, Z. Fabrication and Characterization of Glycogen-Based Elastic, Self-Healable, and Conductive Hydrogels as a Wearable Strain-Sensor for Flexible e-Skin. *Polymer* **2020**, *210*, No. 122961.
(32) Tong, R.; Chen, G.; Tian, J.; He, M. Highly Stretchable, Strain-Sensitive, and Ionic-Conductive Cellulose-Based Hydrogels for Wearable Sensors. *Polymers* **2019**, *11*, No. 2067.
(33) Zhou, Y.; Wan, C.; Yang, Y.; Yang, H.; Wang, S.; Dai, Z.; Ji, K.; Jiang, H.; Chen, X.; Long, Y. Highly Stretchable, Elastic, and Ionic Conductive Hydrogel for Artificial Soft Electronics. *Adv. Funct. Mater.* **2019**, *29*, No. 1806220.
(34) Lai, P. C.; Yu, S. S. Cationic Cellulose Nanocrystals-Based Nanocomposite Hydrogels: Achieving 3d Printable Capacitive Sensors with High Transparency and Mechanical Strength. *Polymers* **2021**, *13*, No. 688.
(35) Wu, J.; Wu, Z.; Lu, X.; Han, S.; Yang, B. R.; Gui, X.; Tao, K.; Miao, J.; Liu, C. Ultrastretchable and Stable Strain Sensors Based on Antifreezing and Self-Healing Ionic Organohydrogels for Human Motion Monitoring. *ACS Appl. Mater. Interfaces* **2019**, *11*, 9405−9414.
(36) Hou, W.; Sheng, N.; Zhang, X.; Luan, Z.; Qi, P.; Lin, M.; Tan, Y.; Xia, Y.; Li, Y.; Sui, K. Design of Injectable Agar/NaCl/Polyacrylamide Ionic Hydrogels for High Performance Strain Sensors. *Carbohydr. Polym.* **2019**, *211*, 322−328.
(37) Li, M.; Chen, D.; Sun, X.; Xu, Z.; Yang, Y.; Song, Y.; Jiang, F. An Environmentally Tolerant, Highly Stable, Cellulose Nanofiber-Reinforced, Conductive Hydrogel Multifunctional Sensor. *Carbohydr. Polym.* **2022**, *284*, No. 119199.
(38) Pan, X.; Wang, Q.; Guo, R.; Cao, S.; Wu, H.; Ouyang, X.; Huang, F.; Gao, H.; Huang, L.; Zhang, F.; Chen, L.; Ni, Y.; Liu, K. An Adaptive Ionic Skin with Multiple Stimulus Responses and Moist-Electric Generation Ability. *J. Mater. Chem. A* **2020**, *8*, 17498−17506.
(39) Yang, B.; Yuan, W. Highly Stretchable and Transparent Double-Network Hydrogel Ionic Conductors as Flexible Thermal-Mechanical Dual Sensors and Electroluminescent Devices. *ACS Appl. Mater. Interfaces* **2019**, *11*, 16765−16775.
(40) Shi, X.; Wu, P. A Smart Patch with On-Demand Detachable Adhesion for Bioelectronics. *Small* **2021**, *17*, 1−11.
(41) Saurav, D.; Mahnan, A.; Konczak, J.*Real Time Voice Activity Detection Using Neck Mounted Accelerometers for Controlling a Wearable*

https://doi.org/10.1021/acsaelm.2c01279
ACS Appl. Electron. Mater. 2023, 5, 205−215

Vibration Device to Treat Speech Impairment; ASME, 2020; pp 7−9. DOI: 10.1115/DMD2020-9081.
(42) Avolio, A. P.; Butlin, M.; Walsh, A. Arterial Blood Pressure Measurement and Pulse Wave Analysis-Their Role in Enhancing Cardiovascular Assessment. *Physiol. Meas.* **2010**, *31*, R1−R47.